



Ice-microsphere templating to produce highly porous nanocomposite PLA matrix scaffolds with pores selectively lined by bacterial cellulose nano-whiskers

J.J. Blaker^{a,*}, K.-Y. Lee^a, A. Mantalaris^b, A. Bismarck^a

^a Polymer and Composite Engineering (PaCE) Group, Imperial College London, South Kensington Campus, London SW7 2AZ, United Kingdom

^b Department of Chemical Engineering and Chemical Technology, Imperial College London, South Kensington Campus, London SW7 2AZ, United Kingdom

ARTICLE INFO

Article history:

Received 27 January 2010

Received in revised form 25 May 2010

Accepted 30 May 2010

Available online 4 June 2010

Keywords:

A. Polymer–matrix composites (PMCs)

A. Nano composites

Bacterial cellulose

ABSTRACT

The production of 3D scaffolds for tissue engineering with provision of a controlled nano-topography remains a significant challenge. Here we have combined an ice-microsphere templating technique with thermally induced phase separation, and by taking advantage of interactions between hydrophilic and hydrophobic phases, lined the pore walls with bacterial cellulose nano-whiskers. The cryogenic technique we have developed not only allows the decoration of the pore walls of 3D porous forms with nano-whiskers but also enables the pore structure, interconnects and surface area to be controlled. Moreover our novel combined solvent extraction and ice sublimation route presented herein preserves the frozen-in structure.

© 2010 Elsevier Ltd. Open access under [CC BY-NC-ND license](http://creativecommons.org/licenses/by-nc-nd/3.0/).

1. Introduction

An important challenge in the development of scaffolds for tissue engineering and cell expansion is in applying nano-scale topography to highly porous 3D forms. Such nano-scale topographies are known to influence cell response, as reviewed in detail elsewhere [1]. The cues the nano-topographical features provide can be key to the survival of cells notoriously difficult to culture, such as haemopoietic stem cells. Haematopoietic stem cell cultures have generated intense interest due to their potential applications in cell-based therapies [2], in particular in the prospective treatment of leukaemia. However, the expansion of these cells is currently limited to two dimensional culture systems, which often require expensive and complex growth factors. Consequently, the utilization of support matrices that afford cells a 3D growth environment by enhancing cell–cell contact, promoting the spatial arrangement of cells, and supporting a high cell density due to their high surface area to volume ratio, has been explored [3–6]. Scaffold parameters such as porosity, interconnectivity and pore size and topography, particularly on the nano-scale are important characteristics that determine cell attachment, growth, and mass transfer [3,7,8]. We have chosen bacterial cellulose nano-whiskers (BCNW), as they inherently possess dimensions in the nano-scale, with diameters between 10 nm and 100 nm and are microscopically similar to collagen fibres, making them appropriate for use as collagen-mimicking components in scaffolds [9,10]. Indeed, the non-woven ribbon of bacterial cellulose resembles the struc-

ture of native extra cellular matrices [9]. BCNW have abundant hydroxyl groups on their surfaces, which are useful sites for functionalization, protein adsorption, act to enhance the wettability of otherwise relatively hydrophobic polymer matrices, such as polylactide (PLA) and can promote cell attachment. Bacterial cellulose has already found application in wound closure and healing [11], drug delivery, vascular grafting [12,13] and as a scaffold material for *in vivo* and *in vitro* tissue engineering [10]. The future prospects of microbial cellulose in biomedical applications have been reviewed in detail elsewhere [9]. In addition to imparting a nanometre scale topography, BCNW have a highly organised hierarchical structure; resulting in high crystallinity (~90%), with a measured Young's modulus of about 114 GPa, comparable to that of glass and aramid fibres [14], making them interesting as fillers in nano-composite materials. Whilst we have produced bacterial cellulose scaffolds via thermally induced phase separation from aqueous solutions and subsequent freeze-drying (unpublished), on immersion in aqueous fluids the hydrogen bonds are disrupted and the scaffolds immediately deform, making them unsuitable for cell culture. We now focus on combining BCNW with PLA as a support matrix and the development of processing techniques to endow 3D porous scaffolds with a lining of cellulose nano-whiskers where they are needed, i.e. at the pore wall surface. In recent work by others [10], efforts have been directed to controlling pore sizes and pore interconnects by cultivating a cellulose producing bacteria, *Acetobacter xylinum*, in the presence of a scaffold of paraffin wax and starch particles of various sizes [10], which can be regarded as a bottom-up approach as the extracellular product cellulose is deposited around the particles in culture. Whilst various groups are working on cellulose reinforced PLA [15,16], there is lit-

* Corresponding author.

E-mail address: j.blaker@imperial.ac.uk (J.J. Blaker).

published on the inclusion of bacterial cellulose in PLA [17], let alone as a material system for use as a scaffold for use in tissue engineering.

Here, we put forward a technique to produce scaffolds of controlled porosity and pore size and more importantly provide nano-scale topography by lining the pore walls with BCNW by exploiting interactions between the hydrophilic and hydrophobic phases. We describe a technique to combine bacterial cellulose with PLA and produce scaffolds using the thermally induced phase separation route, which is built upon by combining with an ice-microsphere templating technique [18]. The ice microspheres act as *in situ* porosifiers and through their size selection and vol.% the scaffold macroporosity can be tuned. The thermally induced phase separation (TIPS) technique enables us to impart a finer controlled porous structure and can facilitate the incorporation of bioactive reinforcement phases [19] and therapeutic drugs [20]. TIPS is attractive as a flexible processing technique, which even enables the production of composite porous microspheres [20–22] and in general of highly porous materials with controlled, interconnected porosity. A downside to the TIPS process is that relatively tortuous interconnects are formed between pores and the pores are generally too small for use in cell culture. To that end, the use of ice microspheres provides further control to achieve larger pores and interconnects depending on the proximity of neighbouring ice-spheres. Further, this work tests the hypothesis that hydrophilic BCNW will be attracted to the polar surface of the ice microspheres and migrate to their surfaces, away from their original dispersion in hydrophobic polymer/solvent solutions to preferentially line the resultant pore walls on removal of the ice. Thereby providing a new tool for decorating the pore walls of 3D macroporous forms with nano-topographical features, where they are required.

2. Materials

Bacterial cellulose was extracted from *nata-de-coco*, a commercially available product, CHAOKOH[®] coconut gel in syrup (Thep. Padung Porn Coconut Co. Ltd., Bangkok, Thailand). Methanol (99.8%), hexane (99%), chloroform ($\geq 99.8\%$), dimethyl carbonate ($\geq 99.0\%$), sulphuric acid (98%) and sodium hydroxide were purchased from Sigma–Aldrich (Poole, UK). All reagents were used without further purification. Poly(D,L-Lactide) (PDLLA) with an inherent viscosity of 1.62 dl g^{-1} was purchased from Purac Biochem (The Netherlands).

3. Experimental

In order to compare the effects of the presence of BCNW and ice microspheres on the resultant scaffolds, three different categories of scaffolds were produced: (i) based on BCNW and PDLLA using dimethyl carbonate (DMC) as the solvent without the presence of ice spheres, these scaffolds served as controls to investigate the effect of BCNW loading on pore structure; (ii) BCNW with PDLLA in the presence of ice microspheres (as *in situ* porosifiers) using chloroform as the solvent, with the solvent extraction (removal of chloroform) conducted in solution using hexane as opposed to freeze-drying, with subsequent freeze-drying to remove the ice; and category (iii), as (ii) however negating the hexane solvent exchange and directly freeze-drying. Categories (ii) and (iii) were developed to exploit hydrophobic and hydrophilic interactions between the phases with the overarching aim to line the pore walls with BCNW. The resultant scaffolds were then subjected to characterization to establish the effect of processing conditions and formulation on their structure, porosity and to determine the location of the BCNW.

3.1. Production of cellulose nano whiskers from *nata-de-coco* and their dispersion in organic solvents

Bacterial cellulose nano-fibrils were extracted in batches of 2.5 kg (net weight) as previously described [22], briefly 2.5 kg of *nata-de-coco* gel cubes (the contents of five jars, equivalent to a cellulose dry weight of $\sim 6 \text{ g}$) were added to 5 l of deionized H₂O (dH₂O) and rinsed several times to remove the majority of the sugar syrup. The cubes were then successively blended at this concentration for 1 min using a laboratory blender (Waring Blender LB20EG, Christison Particle Technologies, Gateshead, UK), homogenized at 20,000 rpm for 2 min (using a Polytron PT 10–35 GT homogenizer, Kinematica, CH) and centrifuged at 14,000 g for 15 min to obtain the blended product [22]. A purification step was then undertaken to remove remaining bacterial debris and soluble polysaccharides [23], whereby the product was dispersed and treated in 0.1 M sodium hydroxide solution at 80 °C for 20 min. Once treated, the dispersion was cooled and subjected to multiple centrifugation and rinse cycles until the reaching pH neutral [22]. A hydrolysis step based on the method previously described by Favier et al. [24] was undertaken in order to obtain cellulose nano-whiskers, as follows. The fibrils were dispersed in dH₂O in a beaker at a concentration of 1 wt.% (with respect to the dry equivalent weight of the cellulose) and sulphuric acid added drop wise to result in an acid to water ratio of 55 wt.%. The solution was continuously agitated and left to hydrolyze at 60 °C for 20 min prior to quenching in dH₂O, and washing back to pH neutral via multiple centrifugation, blending and re-suspension in dH₂O. The hydrolysis of bacterial cellulose using sulphuric acid has been well established [25,26] and the resultant cellulose nano-whiskers well characterized; hydrolysis under such conditions is known to result in BCNW of between 10 and 30 nm diameter and lengths ranging from 100 nm to several microns. In order to produce the composite scaffolds it was necessary to solvent exchange the fluid in which the BCNW were dispersed, through methanol into either dimethyl carbonate (DMC) or chloroform, in accordance to the formulations given in Table 1 for the various scaffold categories. The methodology given below is for chloroform, however, this step is analogous for DMC; the words DMC and chloroform can be interchanged. A suspension of BCNW in water was centrifuged, the supernatant decanted and substituted for methanol to maintain a BCNW to solvent ratio of 10:3 w/v (with respect to the dry equivalent weight of BCNW), this suspension was then homogenized for 3 min to disperse the BCNW in the solvent. The process was repeated four

Table 1

Scaffolds formulations, predicted porosities, measured porosity and surface area measurement by BET.

Sample ID/ category	Ice sphere content [%] ^a	CNW content [wt.%] ^b	Predicted porosity [%]	Measured porosity [%]	BET surface area [m ² g ⁻¹]
Control/ii	0	0	96.0	89.3 ± 2.5	0.65 ± 0.02
Control_50/ ii	50	0	98.0	97.3 ± 0.4	0.93 ± 0.06
A20/ii	20	0.5	96.8	94.8 ± 0.7	1.44 ± 0.04
A50/ii	50	0.5	98.0	96.9 ± 0.5	2.79 ± 0.10
B20/ii	20	2	96.8	95.1 ± 0.2	2.66 ± 0.03
B50/ii	50	2	98.0	97.3 ± 0.1	3.96 ± 0.06
C50/ii	50	5	98.0	96.1 ± 0.2	38.89 ± 0.13
C67/ii	67	5	98.7	– ^e	7.65 ± 0.07
Z0 ^c /i	0	30	96.0	96.2 ± 0.4	–
H20 ^d /iii	20	30	96.8	92.6 ± 0.8	3.10 ± 0.03

^a Relative to the total volume of polymer solution (PDLLA, CNW and chloroform).

^b CNW content, wt.% relative to PDLLA.

^c Sample prepared using dimethyl carbonate as opposed to chloroform.

^d Sample freeze-dried, *without* any solvent exchange in hexane.

^e Sample too fragile for testing.

times with methanol and then four times with chloroform to result in a dispersion of BCNW in chloroform.

3.2. Generation of ice microspheres for use as *in situ* porosifiers

Ice microspheres were formed by freezing a water mist generated from an ultrasonic fogger (Maplin electronics, UK) in liquid nitrogen. The ultrasonic fogger was placed in a water reservoir and the water mist generated blown into a sink of liquid nitrogen whereupon ice microspheres were formed, as depicted in Fig. 1. Sieves were placed into the liquid nitrogen bath prior to microsphere harvesting. On freezing, the spheres sank and were actively sieved due to turbulence in the liquid nitrogen to diameters ranging between 100 and 500 μm , to yield a pore size deemed suitable for cell culture. Whilst attempts were made to spray water directly into liquid nitrogen, the spheres produced were too large and there were few within the desired size range. Immediately prior to incorporation in the formulations (Table 1), the ice spheres were poured into polypropylene (Falcon™) tubes which themselves were pre-cooled in liquid nitrogen, and weighed to determine the desired amount by volume to be added to the formulations.

3.3. Production of the composite scaffolds via TIPS using dimethyl carbonate (scaffold category (i); no ice microspheres)

Scaffold pre-forms were produced by freezing the PDLLA/BCNW and solvent mixtures (as summarized in Table 1), maintaining the polymer:solvent ratio to 5% (w/v). The BCNW content was varied to give either 0 wt.%, 5 wt.%, 30 wt.% or 50 wt.% relative to the PDLLA. The PDLLA was first dissolved in dimethyl carbonate (DMC) in Falcon™ tubes, prior to the addition of BCNW (themselves dispersed in DMC), and the mixture adjusted to maintain the 5% (w/v) PDLLA to solvent ratio. The mixtures were then agitated and ultrasonicated for 15 min in a bath to improve the BCNW dispersion. The mixtures were then transferred into silicon rubber vessels using a spatula, prior to freezing in liquid nitrogen (-196°C). In an effort to induce orientated tubular macropores, the samples were directionally frozen from the bottom up, as described below, these tubular macropores are a well-known feature of the TIPS processing technique [27,28]. The silicon vessels were made from tube of internal diameter 12.5 mm (thickness 3 mm), which were fitted partially over brass cylinders (12.7 mm diameter and 20 mm in height), such that 5 mm of tube was fitted, leaving a fill able volume of 3 ml. The brass cylinder facilitated conduction of the temperature and hence directional freezing. The rubber tubes were partially spliced axially in three places to enable sample removal after freezing. Directional freezing of the mixtures was

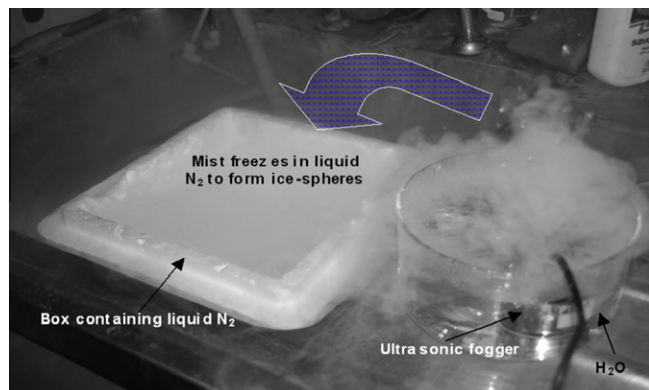


Fig. 1. Set-up used for the generation of ice-microspheres, the arrow represents the movement of the mist, which as fanned manually over the nitrogen; two sieves were placed in the box that contained liquid nitrogen to facilitate the active sieving of the spheres to the size range 100–500 μm diameter.

achieved by placing the bottom face of the brass on a cylinder of steel immersed in liquid nitrogen. Once frozen, the silicon/brass vessels were removed and a sharp knock with a hammer fractured the silicon rubber along the splices and the sample was taken for freeze-drying to remove the solvent.

3.4. Production of scaffolds with BCNW lined pores, using ice microspheres, chloroform as PDLLA solvent and solvent exchange to remove the chloroform (scaffold category (ii))

Scaffold formulations were produced according to Table 1, varying the ice sphere content (relative to the total content) to be between 20 vol.% and 66.7 vol.%. The BCNW content was varied between 0 and 5 wt.% with respect to the PDLLA. A schematic clarifying the processing method detailed here is given in Fig. 2. Formulations consisting of different fractions by weight of BCNW in chloroform were produced by serial dilution. PDLLA was subsequently dissolved into each formulation at a consistent concentration of 5% (w/v) with respect to the chloroform volume. Ice microspheres were then added in a -25°C environment and the slurries (paste-like mixtures) agitated using a metal spatula (also at -25°C) to ensure homogeneous mixing and to expose the BCNW to the ice microsphere surfaces. The mixtures were then transferred to the aforementioned silicon/brass vessels and a thin wire trace (0.5 mm) with a loop (of ~ 3 mm) inserted into the middle of the sample to facilitate hanging of the sample in the solvent extraction media, described further. After freezing and sample removal by fracturing the silicon tube (previously described) the samples were suspended in a bath of cold hexane via the wire traces (attached to a bar overhanging the hexane). Hexane was chosen as a suitable solvent extraction medium as it is a non-solvent for PDLLA, is highly hydrophobic, is miscible with chloroform and has a lower freeze point than chloroform (-95°C , as opposed to -63.5°C for chloroform). The amount of hexane to chloroform was fixed at 98 vol.%, as PLA in chloroform is known to precipitate in hexane at this ratio [20]. The hexane was maintained in a beaker surrounded by dry-ice in a polystyrene foam box, thereby maintaining the temperature of the hexane at -78.5°C ; maintaining the suspended scaffold pre-forms frozen and the hexane liquid. The hexane was gently stirred using a magnetic stirrer in an effort to reduce damage to the suspended samples due to agitation. The dry ice was left to sublime over a period of 48 h, during which the chloroform mixed with the hexane, leaving the PDLLA scaffold/ice microspheres intact. The suspended scaffolds were then removed at -10°C , blotted with filter paper, re-frozen in liquid nitrogen and subsequently freeze-dried to remove the ice-microspheres and obtain the scaffolds.

3.5. Production of scaffolds with BCNW lined pores, using ice microspheres, chloroform as PDLLA solvent and freeze-drying to remove the chloroform and ice microspheres simultaneously (scaffold category (iii))

Scaffold-pre-forms were made according to scaffold category (ii) above, however, instead of precipitating the chloroform in cold hexane solution, the samples (frozen in liquid nitrogen) were then directly freeze-dried under liquid nitrogen for 48 h and then at room temperature for a further 48 h to remove the ice microspheres and chloroform as detailed below, yielding the porous scaffolds. A special freeze-drying apparatus was improvised in order to freeze-dry the sample under liquid nitrogen. Whereby, the sample was placed in a glass lyophilization flask, itself immersed in liquid nitrogen contained in a polystyrene foam box and the lyophilization flask connected to a vacuum pump via a cold-trap, itself immersed in liquid nitrogen to collect (via condensation) the chloroform. After 48 h, the liquid nitrogen surrounding the

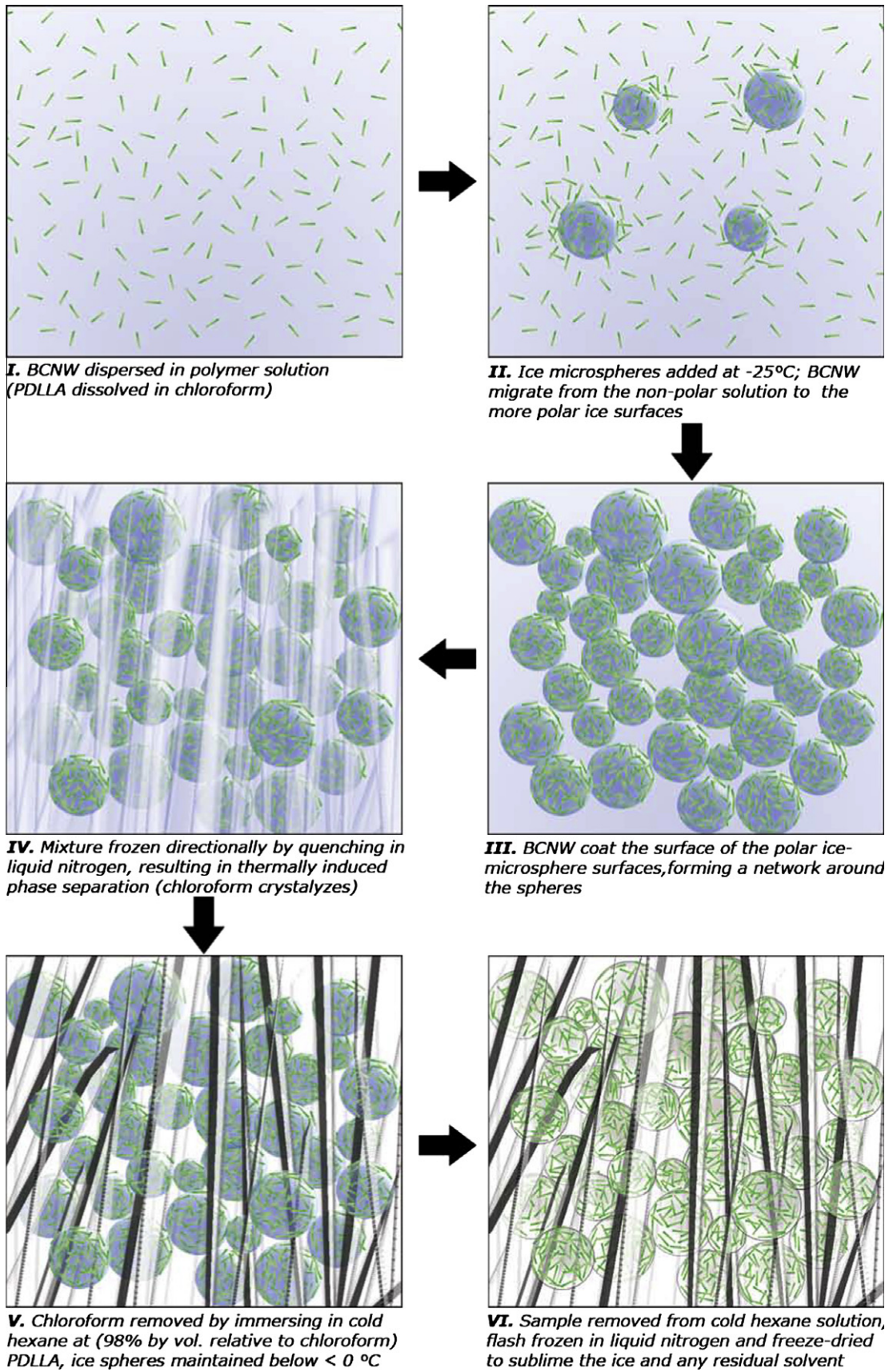


Fig. 2. Schematic of the process used to generate scaffolds with BCNW lined pores of controlled size.

lyophilization flask (the level of which was maintained during this initial period), was allowed to deplete and the sample was allowed

to heat slowly to room temperature, whereupon it continued to be freeze-dried for a further 48 h.

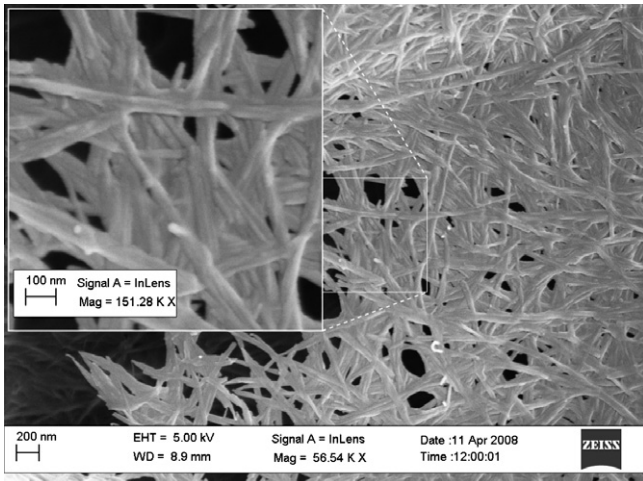


Fig. 3. SEM images of the bacterial cellulose nano-whiskers, shown inset at high magnification.

3.6. Scaffold characterization

3.6.1. Scanning electron microscopy (SEM)

The samples were sectioned in axially (with respect to their cylindrical shape) and then cut radially to give three pieces, images were then taken throughout the interior of the sample to investigate the morphology, assess the distribution and location of BCNW and effect of freeze-direction on sample preparation. At least five different areas per sample were imaged at different magnifications,

using a high resolution SEM (LEO Gemini 1525 FEG-SEM, Oberkochen, D), as previously described [17].

3.6.2. Determination of surface area

The surface area of the polymer foams was determined from nitrogen adsorption isotherms at $-196\text{ }^{\circ}\text{C}$ applying the Brunauer–Emmet–Teller (BET) model. The measurements were performed using a surface area analyser (Micromeritics ASAP 2010). Before performing the gas adsorption experiments, adsorbed impurities were removed via a ‘degassing’ step. Approximately, 1 g of each foam sample was placed inside glass sample cells and purged overnight in a helium atmosphere at a temperature of $40\text{ }^{\circ}\text{C}$. For the analysis part, small amounts of nitrogen (the adsorbate) were admitted into the evacuated sample chamber.

3.6.3. Determination of porosity

The envelope volume was first determined by cutting the samples into cubes $\sim 4 \times 4 \times 4\text{ mm}^3$ and scanning them in two planes at 300 dpi, the pixels were then counted using Adobe Photoshop to determine area in one plane and thickness from the second plane, thereby the product, i.e. envelope volume was determined. Porosity was calculated from the envelope volume, using the known mass of the samples and their solid densities, as previously described in [29]. Three samples were measured per sample type and the predicted porosity calculated by dividing the volume of the total void space (due to the presence of ice spheres and solvent), by the total solid volume (including solid and voids). This method was chosen over mercury intrusion porosimetry as the technique can cause damage and yield erroneous results when applied to highly porous and fragile samples; displacement tech-

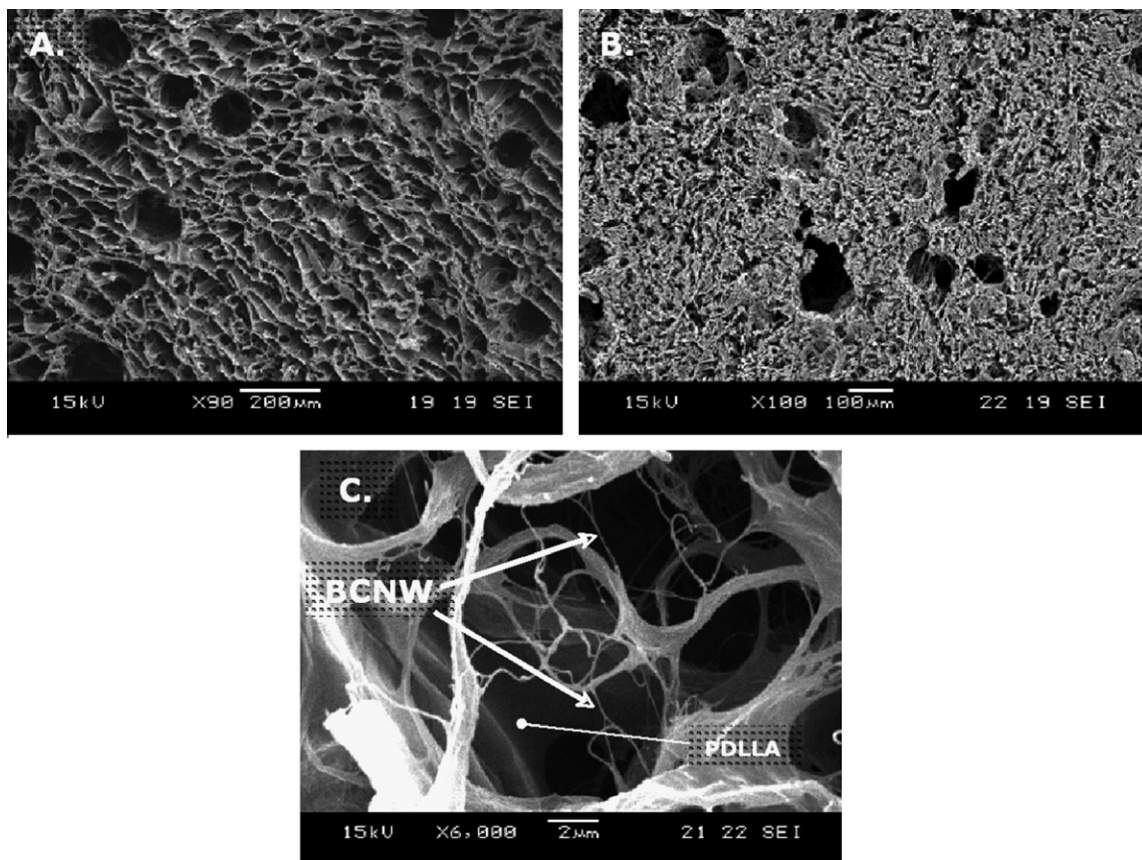


Fig. 4. SEM images of scaffolds produced from PDLLA/BCNW using DMC as solvent without the presence of ice-microspheres. (A) Sample containing 5 wt.% BCNW, in comparison to sample containing $\sim 50\text{ wt.}\%$ BCNW (B), which appears more blocked and less openly porous. (C) SEM image of the 30 wt.% BCNW filled sample, exemplifying the bridging of large PDLLA matrix pores by BCNW, which acting to effectively block the pore to cells, transforming 20–50 μm pores to around 5 μm .

niques were also deemed inappropriate in case either of the phases swelled or closed pores were present.

4. Results and discussion

The use of the ultrasonic fogger proved key to forming a large number of ice microspheres in the desired size range (100–500 μm) and preferred over previous techniques [18,30], which have used rather expensive capillary needles (Eppendorf Femto-tips) and injection systems to achieve almost spherical ice microparticles.

The BCNW used in our study are shown in Fig. 3 (inset at high magnification), it is possible to resolve that the diameter of the whiskers is between 20 and 30 nm, with lengths of up to several microns. The length of the whiskers is harder to resolve due to agglomeration.

Scaffolds produced according to category (i) using DMC as solvent without the presence of ice microspheres were successfully

produced, as shown in the SEM images Fig. 4a–c, loadings of BCNW above 5 wt.% became increasingly viscous, becoming a paste-like consistency at 30 wt.% and almost like wet cotton wool at ~ 50 wt.%. There was little difference in the macrostructure of the control (0 wt.%) and 5 wt.% filled scaffolds, yet at higher loadings, the pore structure appeared less open and interconnected (Fig. 4a vs. b) this is due to the BCNW acting to bridge the pores, effectively blocking them, as exemplified in Fig. 4c. Unlike TIPS scaffolds formed using particles [20,21], the BCNW network acts to bridge the pores, making the scaffolds unsuitable for use in tissue engineering, effectively turning pores of between 20 and 50 μm into pores < 5 μm , as exemplified in Fig. 4c, making it physically impossible for many cells to penetrate the interior network. It was not possible to use DMC as the solvent in combination with ice microspheres as the melt point of DMC (ca. 2–4 $^{\circ}\text{C}$); besides, DMC is partially miscible with water. Chloroform is far more hydrophobic and has a melt point far lower and was therefore selected as a suitable solvent. Whilst DMC is facile to freeze-dry chloroform is problem-

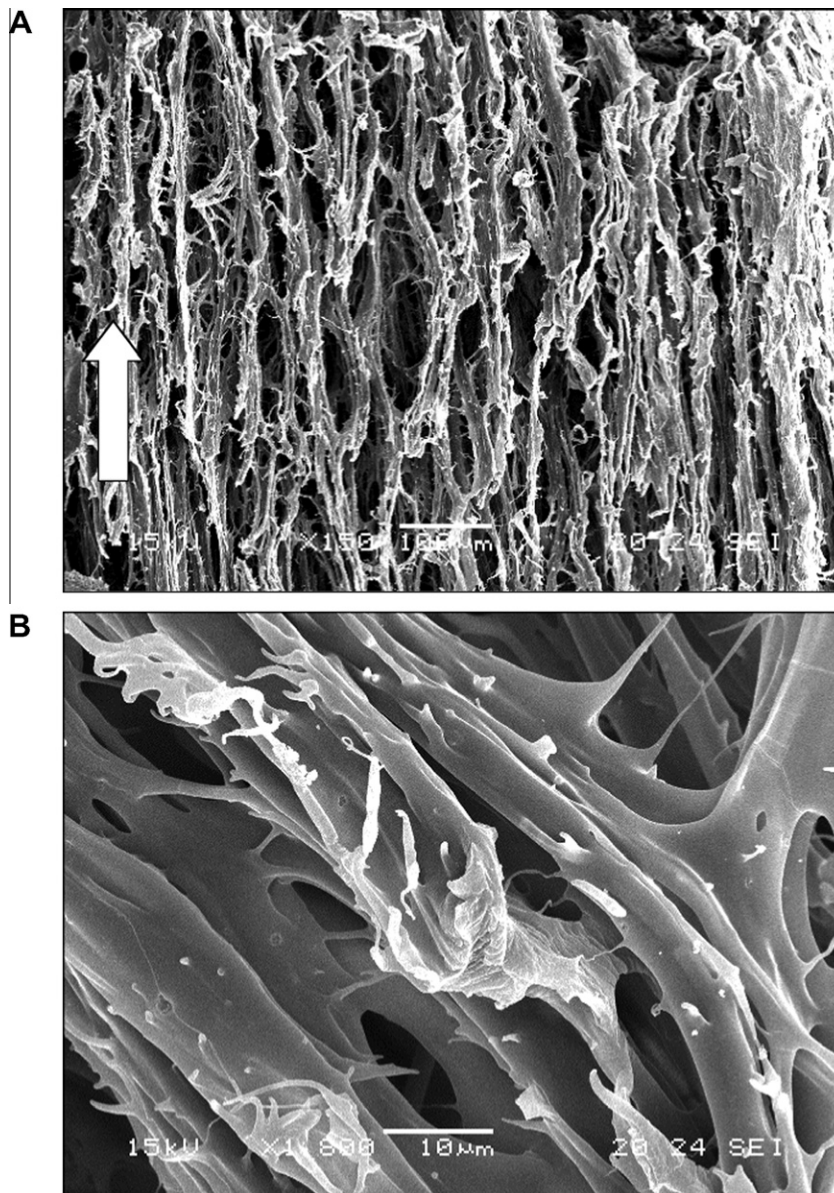


Fig. 5. SEM images of the control scaffold, produced in accordance with category (ii), without bacterial cellulose or ice spheres present. The tubular macropores (shown sectioned) can be seen at low magnification (A), these are directional due to the development of the directional freeze-front (arrowed), the typical ladder-like/tubular TIPS structure is shown at high magnification (B).

atic. For this reason the solvent exchange in cold hexane procedure was developed.

The scaffolds produced according to category (ii) whereby the chloroform solution was exchanged with non-solvent for the PDLLA, hexane, show the typical features of TIPS scaffolds (ladder-like and tubular pore structures), as shown for the control sample (SEM) at high and low magnification, Fig. 5a and b. In the case of the control samples, the tubular macroporous structure can be seen (Fig. 5a), evidenced by the aligned pores due to the directional freezing (indicated by the arrow). Scaffolds produced

in the presence of ice-microspheres according to category (ii) exhibited interconnected pores and features of TIPS (a fine, highly porous network, tubular/ladder-like pore network) and BCNW located at the surface of the pore walls, as shown in Figs. 6a and b and 7a and b, however, the effect of directional freezing not evident. Whilst efforts were made to directionally freeze the samples, this thermodynamic process is difficult to control, especially in the presence of ice microspheres and BCNW, and therefore whilst there was little evidence of tubular macropores, the ladder-like/tubular microstructure characteristic to the TIPS process were

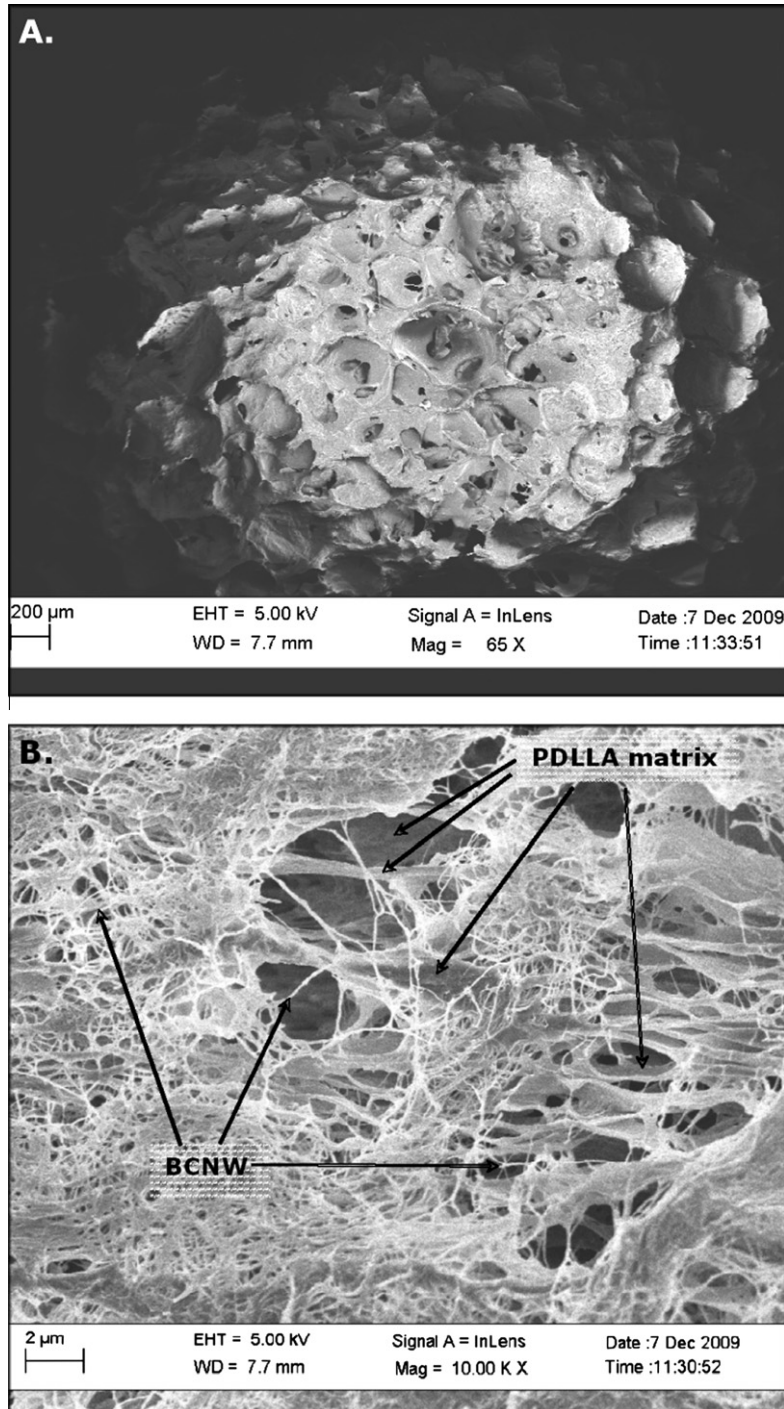


Fig. 6. (A) Scaffold formed by ice-microsphere *in situ* porosifiers and filled with 5 wt.% BCNW with respect to PDLLA. The sample corresponds to formulation with 50 vol.% ice spheres (i.e. formulation C50 in Table 1). (B) High magnification SEM image showing the interior of a pore wall of the same sample, showing a network of cellulose nano-whiskers lining the pore, underneath which is the typical ladder-like TIPS structure of the PDLLA.

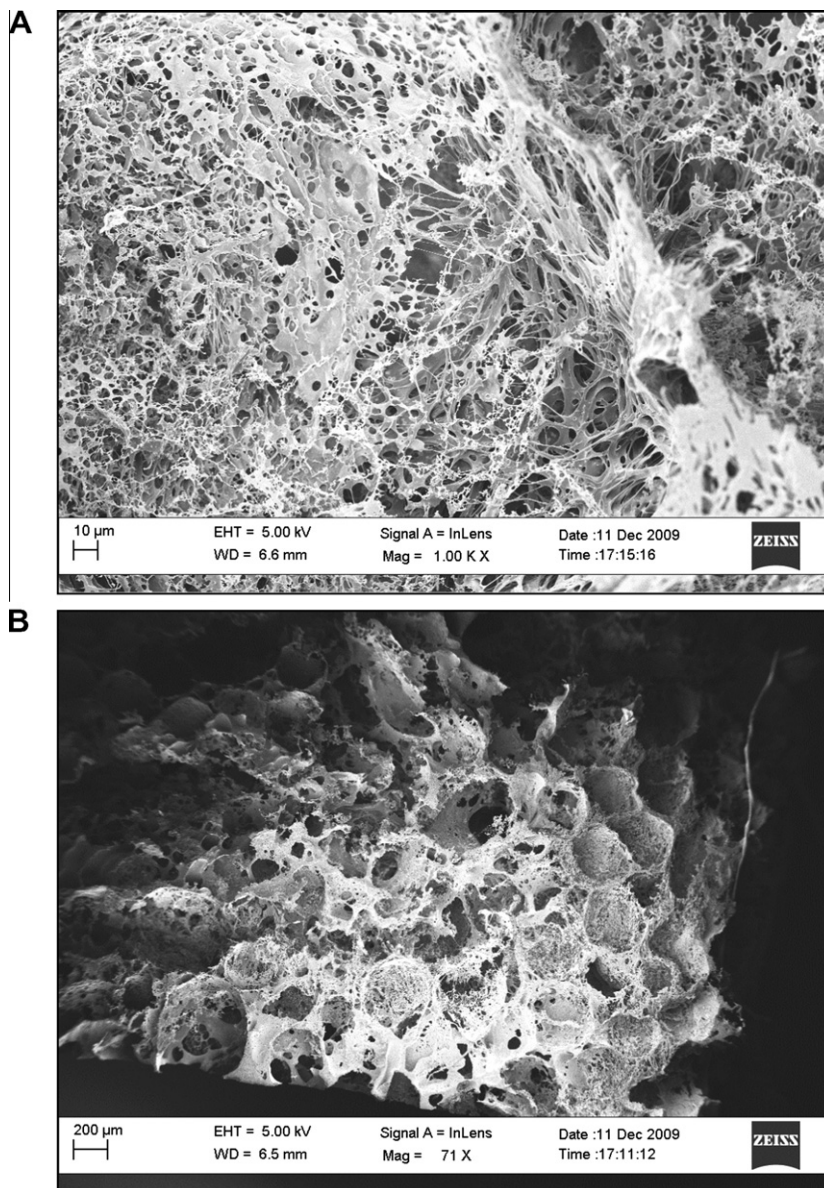


Fig. 7. SEM image of a sample containing 2 wt.% BCNW produced with 50 vol.% ice microspheres (i.e. formulation B50 in Table 1); the BCNW are again shown to line the pore wall and the TIPS tubular/ladder-like structure is preserved underneath; shown at high (A) and low (B) magnification.

present, as shown (SEM, Figs. 6a and b and 7a and b) for samples produced with 50 vol.% ice microspheres and loadings of BCNW at 5 and 2 wt.%, respectively. There was little evidence of BCNW away from the surface of the ice microspheres, with the exception of some bridging spheres due to their tangled network. By combining the TIPS and microsphere technique with solvent extraction in hexane and subsequent freeze-drying, not only were the BCNW located at the surface of the spheres but all the structures frozen-in were preserved. During thermally induced phase separation the solution separates into a solvent rich and solvent poor (polymer rich) regions, the ice-microspheres remain as such during this process. The interconnected frozen solvent crystal network formed is later extracted leaving behind a porous structure, which is a negative of the 3D solvent crystal 'fingerprint'. In the case of the formulations containing ice microspheres as *in situ* porosifiers, spherical pores are left behind. This is contrary to the scaffolds produced according to category (iii) whereby the solvent exchange step was obviated and efforts were made to sublime the chloroform and ice simultaneously. An example of a resultant scaffolds is given

in Fig. 8. Whilst the structure appears appropriate for tissue engineering use, in that the network is highly porous and interconnected, it was obvious that the structure frozen-in during the TIPS processing was not present and that where the PDLLA itself was no longer porous (a thick (75 µm) polymer wall is arrowed in Fig. 8b). We hypothesize that the ice sphere network and high loading of BCNW (30 wt.%) acted to keep the structure together during freeze-drying, whilst the chloroform phase changed from solid to gas via the liquid phase during freeze-drying, partially dissolving the polymer. The polymer walls in the scaffolds produced by others [18,30] via TIPS and freeze-drying of chloroform look similar, in that the TIPS structure has not been preserved, whereas the ice microparticles have acted successfully as *in situ* porosifiers.

All the scaffolds produced were highly porous, as shown in Table 1, with porosities in excess of 94%, even recorded at 97.3% for a sample containing 50 vol.% ice spheres and 2 wt.% BCNW. The high porosities are due to (i) the preservation of the frozen-in, TIPS structure and as a result of the presence of the *in situ* ice microsphere porosifiers; the PDLLA to solvent ratio was maintained at

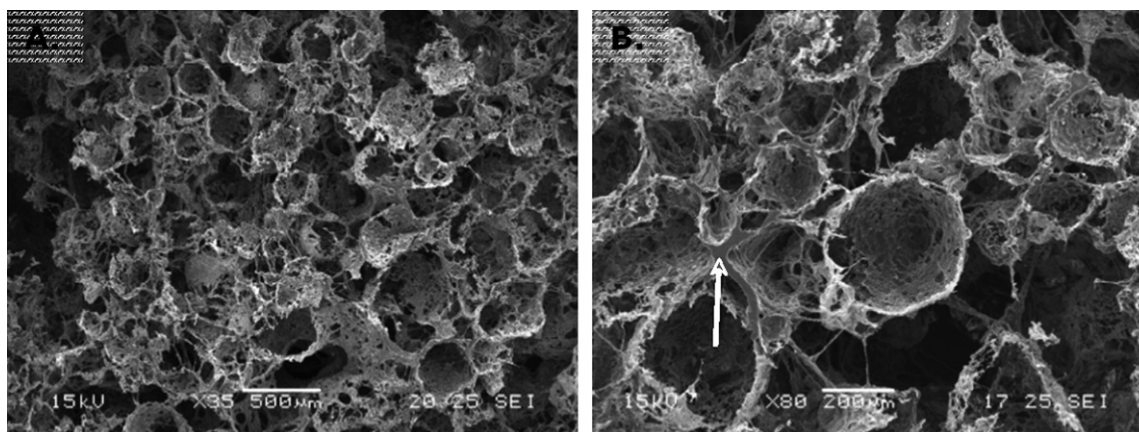


Fig. 8. SEM image of a sample containing 30 wt.% BCNW, produced according to category (iii), using 20 vol.% ice microspheres and freeze-dried without the solvent exchange in hexane. At low magnification: (A) the scaffold appears to be well interconnected, and at high magnification; (B) the smooth polymer wall can be observed (arrowed).

5% (w/v), therefore approximately 95% of the scaffold produced should be expected to be porous as the solvent is removed completely. In the case of the scaffolds produced from category (iii), where the TIPS structure was not preserved well, the porosity is lower than predicted (Table 1). The surface area of the scaffolds was noted to increase with both increased ice microsphere loading and with concentration of BCNW. The method developed according to category (ii) herein allows total control over macro and microporosity, surface area which is enhanced by the BCNW lining the pore walls and their concentration. Surprising there is a near ten fold increase in scaffold surface area in comparing sample codes B50 and C50 (detailed in Table 1) for scaffolds with the same loading of ice (50 vol.%) and only differing in their concentration of BCNW (2 wt.% vs. 5 wt.%), the viscosity of the mixtures is higher with increasing cellulose concentration and there may be some further agglomeration of the cellulose which may be responsible for this increase, which is being further investigated. Whilst the mechanical properties have not been the focus of the current work, it is well known that PLA matrix scaffolds of porosities >92% are fragile [29], yet suitable for withstanding handling, cutting and conditions for cell culture [31]. From handling the materials developed here, those filled with bacterial cellulose were noticeably tougher than PLA matrix only scaffolds and difficult to cut using foil edge razor blades, which tended to blunt quickly due to the stiff cellulose. The scaffold produced from 66.7 vol.% ice spheres, with a theoretical porosity of 98.7% was however too fragile to cut and manipulate and therefore deemed unsuitable as a scaffold. The scaffold produced using 20 vol.% ice spheres, with 30 wt.% cellulose and porosity 92.6% was the scaffold most resilient to handling.

5. Conclusions

We have developed a technique to rapidly produce a large number of appropriately sized ice microspheres through the use of an ultrasonic fogger and evaluated the incorporation of these *in situ* porosifying spheres in combination with scaffolds produced by thermally induced phase separation in the presence of bacterial cellulose nano-whiskers. Whilst it is possible to produce PLA/BCNW scaffolds using traditional TIPS processes the pore morphology is not suitable for the expansion of cells in 3D culture. To this end combining TIPS with ice microspheres and through exploiting hydrophilic–hydrophobic interactions between the polar ice spheres, hydrophilic BCNW and hydrophobic polymer and solvent mixture we have developed a technique to produce scaffolds of controlled porosities up to 97% with spherical interconnected pore

walls lined by BCNW where they are required for direct interaction with cell in culture. It was also necessary to develop a new solvent/ice extraction technique in order to preserve the frozen-in structure and pore morphologies, as the direct freeze-drying of chloroform was otherwise problematic.

Acknowledgements

J.J.B acknowledges the experimental assistance of Aulfa Azman and the EPSRC for funding. This work was supported by the Challenging Engineering Programme (EP/E007538/1) of the UK Engineering Physical Science Research Council (EPSRC).

References

- [1] Kripparamana R, Aswath P, Zhou A, Tang LP, Nguyen KT. Nanotopography: cellular responses to nanostructures materials. *J Nanosci Nanotechnol* 2006;6(7):1905–19.
- [2] Nielsen LK. Bioreactors for hematopoietic cell culture. *Annu Rev Biomed Eng* 1999;129–52.
- [3] Agrawal CM, Ray RB. Biodegradable polymeric scaffolds for musculoskeletal tissue engineering. *J Biomed Mater Res* 2001;55(2):141–50.
- [4] Bagley J, Rosenzweig M, Marks DF, Pykett M. Extended culture of multipotent hematopoietic progenitors without cytokine augmentation in a novel three-dimensional device. *Exp Hematol* 1999;27(3):496–504.
- [5] Banu N, Rosenzweig M, Kim H, Bagley J, Pykett M. Cytokine-augmented culture of hematopoietic progenitor cells in a novel three-dimensional cell growth matrix. *Cytokine* 2001;13(6):349–58.
- [6] Li Y, Ma T, Kniss DA, Yang ST, Lasky LC. Human cord cell hematopoiesis in three-dimensional nonwoven fibrous matrices: *in vitro* simulation of the marrow microenvironment. *J Hematother Stem Cell Res* 2001;10(3):355–68.
- [7] Ma CYJ, Kumar R, Xu XY, Mantalaris A. A combined fluid dynamics, mass transport and cell growth model for a three-dimensional perfused bioreactor for tissue engineering of hematopoietic cells. *Biochem Eng J* 2007;35(1):1–11.
- [8] Tun T, Miyoshi H, Aung T, Takahashi S, Shimizu R, Kuroha T, et al. Effect of growth factors on *ex vivo* bone marrow cell expansion using three-dimensional matrix support. *Artif Organs* 2002;26(4):333–9.
- [9] Czaja WK, Young DJ, Kawecky M, Brown RM. The future prospects of microbial cellulose in biomedical applications. *Biomacromolecules* 2007;8(1):1–12.
- [10] Bäckdahl H, Esguerra M, Delbro D, Risberg B, Gatenholm P. Engineering microporosity in bacterial cellulose scaffolds. *J Tissue Eng Regen Med* 2008;2(6):320–30.
- [11] Czaja W, Krystynowicz A, Bielecki S, Brown RM. Microbial cellulose—the natural power to heal wounds. *Biomaterials* 2006;27(2):145–51.
- [12] Helenius G, Bäckdahl H, Bodin A, Nannmark U, Gatenholm P, Risberg B. *In vivo* biocompatibility of bacterial cellulose. *J Biomed Mater Res* 2006;76A(2):431–8.
- [13] Yamanaka S, Ono E, Watanabe K, Kusakabe M, Suzuki Y. European patent no. 0396344; 1990.
- [14] Hsieh YC, Yano H, Nogi M, Eichhorn SJ. An estimation of the Young's modulus of bacterial cellulose filaments. *Cellulose* 2008;15(4):507–13.
- [15] Liu DY, Yuan XW, Bhattacharyal D, Eastal AJ. Characterisation of solution cast cellulose nanofibre-reinforced poly(lactic acid). *Express Poly Lett* 2010;1(4):26–31.
- [16] Braun B, Dorgan J, Knauss DM. Reactively compatibilized cellulosic polylactide microcomposites. *J Polym Environ* 2006;14(1):49–58.

- [17] Lee K-Y, Blaker JJ, Bismarck A. Surface functionalisation of bacterial cellulose as the route to produce green polylactide nanocomposites with improved properties. *Comp Sci Tech* 2009;69(15–16):2724–33.
- [18] Dong YS, Guo C, Lin PH, Yin LH, Pu YP. Preparation of porous poly(L-lactic acid) (PLLA) scaffold by porogen leaching and freeze drying. *Key Eng Mater* 2005(288–289):381–4.
- [19] Rezwani K, Chen QZ, Blaker JJ, Boccaccini AR. Biodegradable and bioactive porous polymer/inorganic composite scaffolds for bone tissue engineering. *Biomaterials* 2006;27(18):3413–31.
- [20] Blaker JJ, Pratten J, Ready D, Knowles JC, Forbes A, Day RM. Assessment of antimicrobial microspheres as a prospective novel treatment targeted towards the repair of perianal fistulae. *Aliment Pharm Therap* 2008;28(5):614–22.
- [21] Blaker JJ, Knowles JC, Day R. Novel fabrication techniques to produce microspheres by thermally induced phase separation for tissue engineering and drug delivery. *Acta Biomater* 2008;4(2):264–72.
- [22] Blaker JJ, Lee K-Y, Li X, Menner A, Bismarck A. Renewable nanocomposite polymer foams synthesized from Pickering emulsion templates. *Green Chem* 2009:1321–6.
- [23] Toyosaki H, Naritomi T, Seto A, Matsuoka M, Tsuchida T. Screening of bacterial cellulose-producing acetobacter strains suitable for agitated culture. *Biosci Biotechnol Biochem* 1995;59(8):1498–502.
- [24] Favier V, Chaney H, Cavaillé JY. Polymer nanocomposites reinforced by cellulose whiskers. *Macromolecules* 1995;28(18):6365–7.
- [25] Roman M, Winter T. Effect of sulfate groups from sulfuric acid hydrolysis on the thermal degradation behavior of bacterial cellulose. *Biomacromolecules* 2004;5:1671–7.
- [26] Eichorn J, Dufresne A, Aranguren M, Marcovich NE, Capadona JR, Rowan SJ, et al. Review: current international research into cellulose nanofibres and nanocomposites. *J Mater Sci* 2010;45(1):1–33.
- [27] Ma PX, Zhang R. Microtubular architecture of biodegradable polymer scaffolds. *J Biomed Mater Res* 2001;56(4):469–77.
- [28] Guitierrez M, Ferrer ML, del Monte F. Ice-templated materials: sophisticated structures exhibiting enhanced functionalities obtained after unidirectional freezing and ice-segregation-induced self-assembly. *Chem Mater* 2008;20(3):634–48.
- [29] Blaker JJ, Maquet V, Jerome R, Boccaccini AR, Nazhat SN. Mechanical properties of highly porous PDLLA/Bioglass® composite foams as scaffolds for bone tissue engineering. *Acta Biomater* 2005;1(6):643–52.
- [30] Chen G, Ushida T, Tateishi T. Preparation of poly(L-lactic acid) and poly(L-lactic-co-glycolic acid) foams by use of ice microparticulates. *Biomaterials* 2001;22(18):2563–7.
- [31] Helen W, Merry CLR, Blaker JJ, Gough JE. Three-dimensional culture of annulus fibrosus cells within PDLLA/Bioglass (R) composite foam scaffolds: assessment of cell attachment, proliferation and extracellular matrix production. *Biomaterials* 2007;28(11):2010–20.